The follicular fluid metabolome differs according to the endometriosis phenotype

Khaled Pocate-Cheriet, Pietro Santulli, Fatiha Kateb, Mathilde Bourdon, Chloé Maignien, Frédéric Batteux, Sandrine Chouzenoux, Catherine Patrat, Jean Philippe Wolf, Gildas Bertho, et al.

TITLE: THE FOLLICULAR FLUID METABOLOME DIFFERS ACCORDING TO THE ENDOMETRIOSIS PHENOTYPE

AUTHOR NAMES AND AFFILIATIONS

Pocate-Cheriet, K. [1, 2, 3, 6 *]
Santulli, P. [1, 2, 4, 6 *]
Kateb, F. [1, 2, 5 *]
Bourdon, M. [1, 2, 4, 6]
Maignien, C. [1, 2, 4]
Batteux, F. [1, 2, 6, 7]
Chouzenoux, S. [1, 2, 6]
Patrat, C. [1, 2, 3]
Wolf, J.P. [1, 2, 3 †]
Bertho, G. [1, 2, 5 †]
Chapron, C. [1, 2, 4, 6 †]

[1] Université de Paris, Faculté de Médecine. Paris, France
[2] Assistance Publique-Hôpitaux de Paris (AP-HP), Hôpital Cochin (HUPC), Centre Hospitalier Paris Centre, France
[3] Service d'Histologie-Embryologie-Biologie de la Reproduction, Paris, France
[4] Département de Gynécologie Obstétrique II et Médecine de la Reproduction, Paris, France

[5] Laboratoire de Chimie et Biochimie Pharmacologiques et Toxicologiques, UMR 8601-CNRS, Université de Paris, Campus Saint-Germain-des-Prés, 45 rue des Saint-Pères, 75006, Paris, France

[6] Département “Développement, Reproduction et Cancer”, Institut Cochin, INSERM U1016, Université de Paris, Paris, France

[7] Service d’immunologie biologique, Paris, Franc.

[*] Khaled Pocate Cheriet, Pietro Santulli, and Fatiha Kateb contributed equally to this work and should be considered joint first authors.

[†] Jean-Philippe Wolf, Gildas Bertho, and Charles Chapron contributed equally to this work and should be considered joint last authors.

CITY: PARIS COUNTRY: FRANCE

CORRESPONDING AUTHOR:

Dr. Khaled POCATE CHERIET, MD

Service d’Histologie-Embryologie-Biologie de la Reproduction, CHU Cochin

123, Bd Port Royal, 75014 Paris, France

Phone: +33-1-58-41-37-00

Email: khaled.pocate@aphp.fr

ABSTRACT

Research Question: Is there a follicular fluid (FF)**-**specific metabolic profile in deep infiltrating endometriosis (DIE) according to the presence of an associated ovarian endometrioma (OMA) that could lead to the identification of biomarkers for diagnosis and prognosis of the disease?

Design: A prospective cohort study. Proton-nuclear magnetic resonance (^{1}H-NMR) experiments were carried out on 50 FF samples from patients presenting with DIE, associated or not with an OMA, and on 29 FF samples from patients with infertility due to a tubal obstruction. The follicles were aspirated individually.

Results: FF glucose levels were decreased in patients with DIE compared with the controls, whereas the levels of lactate and pyruvate were increased. FF samples from patients with DIE also had higher levels of lipids and ketone bodies. Conversely, the levels of citrate, creatine, and amino acids such as tyrosine and alanine were decreased in FF samples from patients with DIE. When taking into account the presence of an associated OMA in patients with DIE, the metabolic analysis revealed enhanced levels of glycerol and ketone bodies in patients with OMA, indicative of the activation of lipolysis followed by β-oxidation. Conversely, the levels of lactate and pyruvate were increased in patients without OMA, whereas the level of glucose was decreased, highlighting the activation of the anaerobic glycolysis pathway. Differences in the levels of amino acids such as threonine and glutamine were also statistically relevant to discriminate between the presence or absence of OMA.

Conclusions: These results are indicative of a mitochondrial dysregulation in endometriosis phenotypes, with a modified balance between anaerobic glycolysis and β-oxidation in OMA phenotypes that could potentially affect the fertility of patients with endometriosis. Since FF composition has been shown to be correlated with both

oocyte development and the implantation outcome after fertilization, these findings may help explain the high level of infertility observed in these patients.

KEYWORDS:

Endometriosis; Metabolomics; Follicular fluid; Endometrioma; Deep infiltrating endometriosis

INTRODUCTION

Endometriosis is a gynecological disease characterized by ectopic growth of endometrial cells outside the uterine cavity (Sampson, 1927), leading to an estrogen-dependent chronic inflammation environment that can cause pelvic pain and infertility (Chapron *et al*., 2019). Endometriosis affects 10% to 15% of women of reproductive age, approximately 40% of whom are infertile (de Ziegler *et al*., 2010). Different phenotypes of this disease have been described, including superficial endometriosis (SUP), deep infiltrating endometriosis (DIE), and ovarian endometrioma (OMA); the latter is considered to be the most severe form and it has a detrimental impact on ovarian physiology. The occurrence of infertility can be explained by the presence of chronic inflammation and oxidative stress in the pelvic cavity (Santulli *et al.,* 2015*)*. Others have pointed out the negative impact of the disease on oocyte quality, which can cause embryonic development impairment and result in a lower implantation competence (Sanchez *et al*., 2014). Currently, the main selection criteria for oocytes and embryos for in vitro fertilization (IVF) rely on morphological aspects associated with cleavage kinetics; however, these criteria have limited predictive capability (Bromer and Seli, 2008). The development of new, non-invasive, and effective methods to select the embryos most likely to give rise to a favourable pregnancy outcome, therefore, represents a high-priority objective in this field.

Metabolomics, defined as the simultaneous detection and quantification of a large number of low-molecular-weight molecules in different biological matrices, is a powerful method that can be used to study an organism's state; either during normal conditions or in response to perturbations such as environmental factors, drugs, or disease. Various metabolomic techniques have been developed, including mass

spectrometry (MS) and proton–nuclear magnetic resonance (^{1}H-NMR) spectroscopy (Amberg *et al*., 2017; Markley *et al*., 2017). The latter technique has the advantage that it does not result in destruction of the samples, and it can provide a quantitative evaluation with minimal handling (Duarte and Gil, 2012). In recent years, metabolomics has increasingly been used as an approach to gain a better understanding of various pathophysiological mechanisms involved in the onset of diseases.

In the context of infertility, follicular fluid (FF) is one of the most relevant fluids for analysis (Bender *et al*., 2010). Indeed, FF, originating both from plasma and local secretion by cumulus cells, has been shown to be essential for oocyte development (Da Broi *et al*., 2018; Dumesic *et a*l., 2015; Edwards, 1974; Fortune, 1994). Determination of its composition may, therefore, allow identification of biomarkers associated with oocyte quality (Revelli *et al*., 2009). In case of endometriosis, for which a lower oocyte quality has been observed (Garrido *et al*., 2000; Xu *et al*., 2015; Orazov *et al*., 2019), determination of the composition of FF could provide insights into the metabolic pathways involved in the disease and that potentially influence oocyte growth and quality. This could lead to the identification of new biomarkers (Sutton *et al*., 2003; Wallace *et al*., 2012). From this perspective, and considering that the composition of the FF surrounding each oocyte is unique, it is imperative to study the FF of every single follicle.

Few metabolomics studies have focused on the characteristics of FF of patients with endometriosis (Cordeiro *et al*., 2017, 2015; Karaer *et al*., 2019; Marianna *et al*., 2017; Sun *et al*., 2018 Morelli *et al*., 2019). Indeed, only two studies to date have analyzed the FF of a single follicle, and these involved only a small number of samples and did not take into account the severity of the disease (Karaer *et al*., 2019; Morelli *et al*.,

147 2019). These authors highlighted the importance of the anaerobic glycolysis
148 pathway, with increased lactate and pyruvate levels observed in the FF of patients
149 with endometriosis. This is in keeping with previous work carried out using pooled FF
150 samples (Marianna *et al.*, 2017). Other metabolites, such as ketone bodies (KB), also
151 appeared to be particularly relevant for the characterization of endometriosis (Morelli
152 *et al.*, 2019). Given that endometriosis is a heterogeneous condition that probably
153 has variable effects on FF composition, it is crucial to take into account the
154 endometriosis phenotype when evaluating its impact.
155 In this context, the aim of this study was to evaluate the impact of DIE on FF
156 composition, using ^{1}H-NMR-based metabolomics, based on analysis of FF from
157 single oocytes following controlled ovarian stimulation, and to evaluate whether the
158 presence or absence of an OMA affects the FF composition.
159

160 **MATERIALS AND METHODS**

161

162 **Patients**

163 The study population comprised sixteen women who were infertile and who were
164 prospectively enrolled in an assisted reproductive technology (ART) attempt at our
165 center between March and June 2018. The women were divided into two groups (an
166 endometriosis group and a control group).
167 The endometriosis group comprised nine women presenting with DIE, some with and
168 some without an OMA. The study data were stored in a prospectively managed
169 database and subsequently used for the analysis. Each patient's personal history
170 was obtained during a face-to-face interview, supplemented by items recorded using
171 a structured questionnaire (Chapron *et al.*, 2010b). The data items collected included

(Chapron *et al*., 2010a) age, parity, gravidity, height, weight, body mass index (BMI), existence and duration of infertility, lifestyle habits, history of hormonal and/or surgical treatments for symptomatic endometriosis, and the existence of gynecological pain symptoms (dysmenorrhea, deep dyspareunia, non-cyclic chronic pelvic pain (NCCPP)), and gastrointestinal and lower urinary tract symptoms. All of the women with endometriosis underwent an appropriate pre-ART imaging workup to obtain a clear diagnosis and staging of the disease. For the DIE and OMA phenotypes, previously published imaging criteria using transvaginal ultrasound (TVUS), magnetic resonance imaging (MRI), or transrectal ultrasonography (Guerriero *et al*., 2016; Guerriero *et al*., 2018; Nisenblat *et al*., 2016; Van den Bosch and Van Schoubroeck, 2018).

The control group comprised seven women for whom the infertility was due to a tubal obstruction only, with no other associated pathological context, such as inflammation or infection. Both groups were not associated with any male infertility factors, and all of the semen parameters were normal according to the World Health Organization (WHO) criteria (WHO, 2010). Women who were more than 42 years of age, exhibited a chronic viral infection, or who had already been included in another ART research protocol were excluded from the study.

All of the enrolled patients provided written informed consent and the study was approved by the relevant Ethical Committee, “Comité de Protection des Personnes” (CPP-2017-32), and registered at Clinicaltrials.gov (EndOvo, NCT03241329).

Controlled ovarian stimulation protocol

The following controlled ovarian stimulation (COS) protocols were performed according to our institutional clinical protocols, using 150–450 IU/day of recombinant

197 follicle-stimulating hormone (rFSH) (Puregon, MSD, Courbevoie, France; Gonal-F,
198 Merck-Serono, Lyon, France) and human menopausal gonadotropin (hMG)
199 (Menopur, Ferring Pharmaceuticals, Gentilly, France) (Bourdon *et al*., 2017). Final
200 oocyte maturation was triggered when ≥3 ovarian follicles with a diameter of ≥17
201 mm were visible by ultrasound and when the estradiol (E2) levels were ≥1.000
202 pg/mL. Final oocyte maturation was achieved using either a single injection of 0.2 mg
203 gonadotropin-releasing hormone (GnRH) agonist (Triptoreline, Decapeptyl, Ibsen
204 France) or 250 µg of recombinant human chorionic gonadotropin (rhCG) (Ovitrelle,
205 Serono, France). Oocyte retrieval was performed 35 to 36 hours later by transvaginal
206 aspiration under ultrasound guidance.
207
208 **Collection and processing of FF samples**
209 The main objective during the ovarian collection was that the entire content of each
210 follicle was aspirated individually into a single dry sterile tube pre-heated to 37 °C
211 while avoiding any blood contamination. After each follicle aspiration, the puncture
212 syringe and the tubing were washed before the next follicle was processed in the
213 same way. Only FF containing a single oocyte were retained for the study; FF that
214 did not contain an oocyte or that contained more than one oocyte were excluded
215 from the study. FF samples that were free of blood contamination were centrifuged at
216 300 x g for 10 min and the supernatants were aliquoted and stored at -80 °C until they
217 were analyzed.
218 The samples were not randomized during the collection but were instead collected as
219 groups and not at the same time of day. All of the included patients had fasted before
220 the oocyte collection took place under local or general anesthesia.
221

Sample preparation

The samples were randomly mixed prior to the NMR measurements, with the aim of mixing the running order of the two groups and thus avoid systematic error measurements. The ^{1}H-NMR experiments were carried out using whole samples without any extraction. Prior to the NMR measurements, the FF samples were thawed on ice. For each NMR sample, 500 µL of FF was added to 50 µL of a solution containing 1 mM sodium trimethylsilylpropionate salt (TSP), which was used as the ^{1}H-NMR chemical shift reference of -0.016 ppm, dissolved in D_2O, used as a field-frequency lock. A total volume of 550 µL was then transferred into 5-mm NMR tubes for analysis.

Spectral acquisition and processing

The ^{1}H-NMR spectra were obtained with a 500 MHz Bruker Avance spectrometer equipped with a 5-mm ^{1}H/^{13}C dual cryoprobe using a SampleXpress^{TM} automated sample changer. A Carr-Purcell-Meiboom-Gill (CPMG) pulse sequence (Meiboom and Gill, 1958) with a spin-echo delay of 400 µs was used to remove any broad peaks originating from macromolecules. For each experiment, after a delay of 5 min for temperature equilibration at 300 K, a total of 512 scans were acquired with 32 768 points and an acquisition time of 1.6 s. A recycle delay of 2 s and a chemical shift spectral window of 20.65 ppm were used, resulting in a total experiment time of 33 min. The ^{1}H-NMR spectra were processed using Topspin 3.1 software (Bruker, GMBH, Karlsruhe, Germany). A zero-filling to 65 536 points with an exponential anodization function using a line broadening of 0.3 Hz was applied prior to Fourier transformation. The spectra were then manually phased and baseline corrected. The spectra were aligned before bucketing, and ultimately the alanine methyl group signal

was used as a chemical shift reference at 1.47 ppm, instead of the TSP signal, which is known to vary in the presence of proteins or lipoproteins. Each metabolite was assigned using Chenomx NMR suite 7.1 software (Chenomx Inc., Edmonton, Canada), the human metabolome database (HMDB) (Wishart *et al*., 2007), and previously published data (Piñero-Sagredo *et al*., 2010).

Spectral bucketing was carried out using the variable size bucketing (VSB) method, as implemented in NMRProcFlow (Jacob *et al*., 2017). This method allows the spectra to be manually divided into unevenly spaced buckets of different sizes to avoid peaks lying in different consecutive integration regions. Only spectral regions corresponding to metabolite signals were included in the analysis. A total of 215 buckets was obtained and further integrated to build the matrix of variables used in the statistical analysis. This matrix of variables was pretreated using MetaboAnalyst (Chong *et al*., 2018; Xia *et al*., 2009) before performing the statistical analysis. Constant sum normalization (CSN) was first applied to account for any differences in sample concentration. Finally, Pareto scaling (Eriksson *et al*., 2004) was used to avoid enhancing background noise and to reduce the importance of large fold changes compared to small ones, while staying closer to the original data (van den Berg *et al*., 2006).

Statistical analysis

All of the clinical data were compiled in a computerized database and analyzed using IBM® SPSS® Statistics version 23.0 software (SPSS Inc. Headquarters, USA). We used the Mann–Whitney U test for the quantitative variables and Fisher's exact test or Pearson's chi-square test for the qualitative variables, as appropriate. A p-value < 0.05 was considered to be statistically significant.

Conventional metabolomics analysis, comprising both univariate and multivariate analysis, was carried out to identify metabolites statistically relevant for discriminating between the groups being studied. Univariate analysis, which deals with each variable one at a time, was performed using the Student's *t*-test for comparisons between two groups, and one-way ANOVA was used for comparisons among more than two groups, using MetaboAnalyst (Chong *et a*l., 2018; Xia *et al*., 2009). Metabolites were considered statistically relevant when their p-value was < 0.05.

Multivariate analysis, which considers all variables simultaneously, was performed using SIMCA software (Sartorius Stedim Biotech). Both principal component analysis (PCA) and supervised orthogonal projections to latent structures discriminant analysis (OPLS-DA) (Trygg and Wold, 2002) were carried out. The latter, taking into account the class of the different samples, was used to maximize class discrimination. The quality of the models thus obtained was assessed according to the usual quality factors, i.e., the cumulative explained variance of observed data X, R^2X; the cumulative explained variance of group assignment Y, R^2Y; and the estimate of predictive ability, Q^2. The goodness of fit of the models was further evaluated using CV-ANOVA (Eriksson *et al*., 2008), with a p-value < 0.05 considered to be statistically significant. Variables responsible for the class discrimination in the OPLS-DA models were identified with the variable importance on projection (VIP) values. The VIP values correspond to the variable weights in the discrimination observed in the model. A VIP score threshold of 1 was used in our study to consider the variables relevant in the group separation. Important metabolites for the classification model were further identified using the S-line plot generated from SIMCA (Figure A in the Supplementary files). The S-line plot is a spectra-like plot colored according to the correlation coefficient (p(corr)) between each variable and

the classification score of the OPLS-DA model (right vertical axis). The more it tends to the red, the more important the metabolite is for separation of the two groups in the corresponding model. It also allows visualization of the covariance (p(ctr)) between each variable and the classification score of the OPLS-DA model, although it is less interpretable since its magnitude is scale-dependent and affected by the intensity of the signal according to the noise level. Important metabolites for the discrimination between the two groups should have a clear covariance as well as a high absolute value of the correlation coefficient.

RESULTS

Study population

Nine women with DIE and seven control patients with a tubal obstruction were included in our study, resulting in a total of 50 and 29 FF samples, respectively. Of the nine patients with DIE, five had an associated OMA, corresponding to 25 samples. The patients' characteristics are presented in Table 1. No significant differences were noted in terms of age, BMI, parity, gravidity, type and length of infertility, or ovarian reserve. The follicular volume and the total retrieved oocytes were also similar in both groups. When taking into account the endometriosis group, the baseline characteristics of the OMA+ and the OMA- DIE patients were also similar, and there were no significant differences between them (Table 2).

Follicular fluid profiles of patients with DIE compared with controls

An untargeted ^{1}H-NMR-based metabolomics approach was used to obtain an overall profile of the FF composition in patients with DIE and in control patients. This

procedure allows identification of metabolites present at different levels in the two groups, with no prior knowledge of those that are potentially relevant. Figure 1 shows a typical ^{1}H-NMR spectrum of FF from a patient with DIE, with the assignment of the most relevant metabolites indicated above their corresponding peaks. These metabolite peaks corresponded to glucose, pyruvate, lactate, lipids, and ketone bodies (KB), and they were statistically relevant for discriminating between the DIE and the control group in the univariate analysis. The Student's *t*-test results indicated that the glucose levels were significantly lower in the patients with DIE compared with the glucose levels in the control patients, whereas the levels of lactate and pyruvate were increased (Figure 2A). The FF of the patients with DIE also had higher levels of lipids and KB, i.e., acetoacetate, 3-hydroxybutyrate, and acetone, as well as threonine (Figure 2B). Conversely, the levels of citrate, creatine, and amino acids such as tyrosine and alanine were lower in the FF of patients with DIE (Figure 2C).

Supervised multivariate analysis led to a clear separation between the two groups, as demonstrated by the OPLS-DA score plot shown in Figure 3A. The quality of the corresponding model was validated through the high-quality factors obtained, $R^2X = 0.839$, $R^2Y = 0.844$, and $Q^2 = 0.697$, as well as the p-value (6.93×10^{-13}) obtained from the CV-ANOVA analysis of the model. The variables responsible for discrimination between the two groups were plotted as a VIP score plot, shown in Figure 3B, and sorted according to their weight in the model. The corresponding most relevant metabolites were the same as those obtained in the univariate analysis, further confirming their importance for discriminating between the FF composition in patients with and without DIE.

Follicular fluid profiles of patients with DIE as a function of the presence or absence of OMA

Interestingly, the OPLS-DA score plot presented in Figure 3A also showed two clusters within the endometriosis group, which corresponded to the presence (OMA+) or the absence (OMA-) of endometrioma. We, therefore, decided to look at differences in FF composition according to the endometriosis phenotypes, since each analysis from the OMA+ and the OMA- DIE patients was made between them. The difference between the OMA+ and the OMA- DIE patients was first assessed by univariate analysis, which revealed the importance of several metabolites for discriminating between the two groups. Among these metabolites, KB and glycerol were present at increased levels in the OMA+ patients (Figure 4A). Conversely, the levels of lactate and pyruvate were increased in the OMA- patients, whereas the level of glucose was decreased (Figure 4B). Some amino acids were also statistically relevant for discriminating between the two groups, with isoleucine levels being increased and alanine, glutamine, and tyrosine levels markedly decreased in the OMA+ phenotype. Interestingly, high levels of threonine and glutamine were biomarkers of the OMA- phenotype. The levels of succinate were also higher in the OMA+ patients. Finally, the creatine and succinate levels were decreased in the OMA- patients (Figure 4C). The OPLS-DA score plot revealed a clear separation between the three groups (Figure 5), the model being validated with a p-value = 1.9×10^{-14}, obtained from a CV-ANOVA analysis.

DISCUSSION

Our study confirms the difference in FF composition between patients with endometriosis and control patients, while also showing that there is a specific metabolic signature according to the endometriosis phenotype. We found that the glucidic balance in the FF of women with endometriosis differed from that in the women in the control group, with a decrease in glucose levels and an increase in pyruvate and lactate levels observed in the FF of patients with endometriosis. A lower concentration of several amino acids was also noted in the presence of the disease. Concurrently, we found that the concentrations of KB and free fatty acids (FFA) were higher in the FF of women with endometriosis. Finally, and for the first time, we showed that the FF of patients with OMA also exhibited specific metabolic profiles when compared with the profiles of endometriosis patients without OMA.

Using a non-targeted ^{1}H-NMR metabolomics approach, the present study highlighted the importance of energetic pathways in the characterization of FF of patients with endometriosis. Indeed, the FF samples from these patients exhibited a decrease in glucose levels, whereas the levels of lactate and pyruvate were increased. These three metabolites are associated with glycolysis, which has been shown to provide a source of energy for oocyte growth (Boland *et al.*, 1994; Piñero-Sagredo *et al.*, 2010). Thus, it appears that this pathway is more active in endometriosis patients. Endometriotic cells are characterized by higher energy needs and they display properties comparable to those of cancer cells (Maignien *et al.*, 2019; Wingfield *et al.*, 1995), and the enhanced level of glycolysis could hence arise from the well-known Warburg effect (Warburg, 1956), thereby allowing for rapid cell proliferation.

These observations are in agreement with the decreased alanine levels seen in the FF from patients with endometriosis, which is consistent with other studies (Marianna *et al.*, 2017). Alanine can be converted into pyruvate, thereby shifting the anaerobic

glycolysis pathway toward lactate production. The decreased level of alanine is, therefore, consistent with an increased level of both pyruvate and lactate. Since alanine has been shown to increase meiotic maturation, the level at which it is present could be important for oocyte development (Cetica *et al.* 2007). To provide a better understanding of how these metabolic changes are interconnected, the pathways potentially affected by endometriosis are presented schematically in Figure 6.

Enhanced glycolysis could also be due to an increase in granulosa cell (GC) activity as a response to the increased need for energy in the rather low oxygen environment in patients with endometriosis (Gull *et al*., 1999; Redding *et al*., 2008; Sutton *et al*., 2003). On the other hand, the accumulation of lactate and pyruvate could also reflect the dysfunction of cellular respiration in mitochondria, as has been observed in endometriosis tissue (Atkins *et al*., 2019). This is supported by the observation of higher levels of threonine (Noster *et al*., 2019) in endometriosis FF samples, which probably reflects an accumulation of this essential amino acid that may no longer be able to enter the tricarboxylic acid (TCA) cycle. Citrate, which is an intermediate in the TCA cycle, is present at a decreased level in endometriosis FF, further supporting this hypothesis.

The reduced activity of mitochondrial respiration in endometriosis could potentially arise from the hypoxic conditions observed during the establishment of the disease (Hsiao *et al*., 2015), or from defective mitochondria (Hsu *et al*., 2015; Atkins *et al*., 2019; Xu *et al*., 2015). Oxidative stress (OS) can also have a deleterious effect on mitochondrial function (Wang *et al*., 2013), while reactive oxygen species (ROS) may exert a negative feedback effect on the TCA cycle. Since endometriosis is associated with OS (Donnez *et al*., 2016; Jana *et al*., 2013; Ngô *et al*., 2009; Santulli *et al*., 2015;

Scutiero *et al.*, 2017), which has also been shown to affect the composition of endometriosis FF (Regiani *et al.*, 2015; Sanchez *et al.*, 2017; Scutiero *et al.*, 2017), the metabolic switch to anaerobic glycolysis observed in endometriosis could be linked to enhanced OS. This is in agreement with previous observations of endometriosis serum samples (Jana *et al.*, 2013).

We also observed a higher level of KB and FFA in patients with endometriosis. The main KB production pathway, mediated by the action of lipases, is activated when glucose levels are not sufficient to meet the energy needs of cells. KB are indeed the final products of lipid metabolism, via their degradation into FFA, followed by β-oxidation leading to acetyl-CoA, which is one of the substrates of the TCA cycle. If the amount of acetyl-CoA is too high, or if the TCA cycle is dysfunctional, acetyl-CoA is diverted to the formation of KB (Dhillon and Gupta, 2020; Fukao *et al.*, 2004; Kerner and Hoppel, 2004; Owen and Hanson, 2004). Conversion of tyrosine into acetoacetate could also contribute to KB production (Knox, 1955; Knox and LeMay-Knox, 1951), which is consistent with the lower level of tyrosine observed in FF samples of patients with DIE. However, in a non-pathological situation, KB are mainly produced in the mitochondria of liver cells and certain other cells, e.g., human astrocytes (Guzmán and Blázquez, 2004; Le Foll and Levin, 2016). The presence of KB in the FF, therefore, raises an intriguing question. Either these compounds can be produced locally in the FF, or they come from blood exchange in patients. Interestingly, we recently reported an abnormally high level of KB in the blood of patients with endometriosis (Maignien *et al.*, 2020). It is also interesting to note that some cancer cells have the remarkable ability to adapt their metabolism to produce KB (Martinez-Outschoorn *et al.*, 2012). Therefore, it can be hypothesized that endometrial cells are similarly capable of producing KB. In addition to their role as

energy-rich compounds, KB have been shown to play a role in promoting inflammation (Chriett *et al*., 2019; Kurepa *et al*., 2012; Shi *et al*., 2014) as well as OS (Cheng *et al*., 2019; Kanikarla-Marie and Jain, 2015; Shi *et al*., 2016), so it is perhaps not surprising that their levels can increase during endometriosis, consistent with the inflammatory and oxidative character of this disease. Interestingly, citrate, the metabolism of which is also associated with oxygen radical production and inflammation (Convertini *et al*., 2016; O'Neill, 2011; Williams and O'Neill, 2018), also exhibited a statistically lower level in endometriosis FF, thus suggesting enhanced cytosolic degradation in patients with endometriosis.

Finally, we also noted a lower level of creatine in endometriosis FF. Creatine is the result of an alternative lipid metabolic pathway via choline. Its lower level could support the shift of lipid metabolism toward β-oxidation; although it could also indicate a higher degree of conversion into phosphocreatine, which is considered to be an energy reserve. Taken together, these results support the hypothesis of a decrease in mitochondrial respiration in endometriosis in favor of other energetic pathways, such as anaerobic glycolysis and lipid metabolism (Figure 6).

OMA presence (OMA+) vs OMA absence (OMA-) in patients with DIE

Interestingly, the multivariate analysis carried out on the results of FF samples from the patients with DIE and the control group highlighted the presence of two clusters in the endometriosis group, corresponding to the presence or absence of OMA. Given that the presence of an associated OMA is a marker for the severity of DIE (Chapron *et al*., 2009), we observed a linear variation in the levels of a number of molecular entities that corresponded to the seriousness of the disease, thus suggesting that these metabolites could potentially be used as biomarkers in FF. The

levels of KB increased monotonically, thus implying an increased predilection towards β-oxidation as an energetic pathway in OMA+. The increased level of glycerol (released during lipid metabolism) is in keeping with this hypothesis. We support the notion that in the presence of OMA, the high energy requirements of highly proliferative endometriotic cells preferentially activate the KB production pathway. This could be explained by the higher levels of estradiol seen in patients with OMA (Huhtinen *et al*., 2012), which has been shown to stimulate the activity of lipases (Cox□York *et al*., 2017; Palin *et al*., 2003). On the other hand, the OMA- FF samples had lower levels of glucose and higher levels of lactate and pyruvate, which could either arise from blood circulation or from local secretion and metabolic processes_(Gosden *et al*., 1988), thus suggesting that OMA- relies on anaerobic glycolysis, which may reflect a less functional TCA cycle in OMA- patients. This is further supported by the finding that levels of succinate, an intermediate in the TCA cycle, are decreased, whereas threonine, which would no longer be able to enter the TCA cycle, accumulates more in OMA- than in OMA+ patients.

The increased level of creatine in the OMA+ patients compared with its level in the OMA- patients could arise from a higher rate of conversion of phosphocreatine into creatine through the action of creatine kinases (CK), thereby fulfilling the high energy needs of endometrioma cells. This could be seen as a parallel with certain invasive cancer cells, in association with increased CK activity (Zarghami *et al*., 1996). CK activity also depends on E2 levels (Fournier *et al*., 1996); these have been shown to be higher in ovarian endometriosis cases (Huhtinen *et al*., 2012), which is consistent with the higher level of creatine observed in OMA+ patients.

Interestingly, glutamine levels appeared to be lower in OMA+ compared with the levels in OMA- patients. Glutamine metabolism is known to support inflammation

(Calder and Yaqoob, 1999) as well as rapid cell proliferation in cancer (Hosios *et al.*, 2016; Yuan *et al.*, 2015), and could be activated by a high estrogen concentration (Zhou *et al.*, 2019). The glutamine level is thus expected to decrease in the presence of an OMA, which is also associated with a high concentration of inflammatory molecules (Ohata *et al.*, 2008; Sanchez *et al.*, 2014). Altogether, these data suggest different energetic pathways are in use according to the DIE phenotype. Whereas DIE without OMA appears to mainly rely on glycolysis, DIE in the presence of OMA appears to rely on other energetic pathways, such as the KB and glutamine metabolism pathways, in a similar way to cancer cells.

Strengths and limitations of the study

The main strengths of this study lie in the novelty of the subject and the methodological design: (i) To the best of our knowledge, this is the first study to focus on the effect of endometriosis on FF composition using a relatively high number of samples obtained single follicular aspirations, with each FF sample having its own oocyte. Only two studies with a similar design have been performed to date, and they used fewer samples, with only one to three follicles individually aspirated (Karaer *et al.*, 2019; Morelli *et al.*, 2019), whereas we analyzed 79 samples. (ii) To the best of our knowledge, this is the first study reporting a difference in FF composition according to the precise endometriosis phenotype, i.e., DIE with the presence or absence of associated OMA. (iii) Only patients who had undergone a thorough imaging exploration of their pelvic cavity were included, and thus their endometriosis status was assessed with a high degree of precision according to strict, previously published imaging criteria (Guerriero *et al.*, 2016; Guerriero et al., 2018; Nisenblat *et al.*, 2016; Van den Bosch and Van Schoubroeck, 2018). Given the heterogeneous

nature of the disease, we selected patients with well-defined phenotypes and we used the surgical classification (SUP, OMA, or DIE), which describes the endometriosis phenotype more accurately than the rAFS classification (the rAFS can include different types of endometriotic lesions at the same stage, including SUP, OMA, and DIE) (Chapron *et al.*, 2019). (iv) Finally, we employed statistical analyses using an untargeted approach, measuring and comparing many metabolite signals simultaneously, to identify those involved in the disease, with no prior knowledge of which might be relevant.

However, our study has some limitations, the main one being the fact that the patients with endometriosis included in our evaluation had the most severe form of the disease. This is due to the specific nature of the patients encountered in our institution, which is a reference center for endometriosis. As endometriosis is a heterogeneous condition, its effect on FF composition may differ according to the condition's degree of severity. We also acknowledge that there is no ideal control group for studying FF metabolic profiles in women with endometriosis (Zondervan *et al.*, 2002). An ideal control group would consist of women who were not infertile and who lacked any other gynecological conditions. Our control group comprised women who underwent ART for tubal obstruction. These women could hypothetically also exhibit altered FF metabolomic profiles, for unknown reasons. In this context, any associations could hence have been underestimated.

CONCLUSIONS

The effect of endometriosis on FF was well documented, as was the characterization of biomarkers that can be used to discriminate between the different phenotypes.

These biomarkers are mainly involved in different energetic pathways and they could reflect a mitochondrial dysfunction in endometriosis that may potentially affect the fertility of patients with endometriosis (Xu *et al.*, 2015). Interestingly, different energetic pathways are activated according to the endometriosis phenotype. The absence of endometrioma appears to result in a reliance on glycolysis, whereas the presence of endometrioma results in a reliance on lipid and glutamine metabolism as an energy supply, in a very similar way to cancer cells.

Since FF composition has been shown to be correlated with both oocyte development and the implantation outcome after fertilization (O'Gorman *et al.*, 2013; Wallace *et al.*, 2012), these findings may help explain the high level of infertility observed in these patients.

However, a further step remains, namely to correlate these results with oocyte quality, embryo quality, and development, which would then represent a new tool for predicting the chance of a pregnancy with a favorable outcome.

Authors' roles

K.P.C. designed the study, interpreted the data, wrote and revised the manuscript, and approved the final draft. P.S. designed the study, analyzed and interpreted the data, revised the manuscript, and approved the final draft. F.K. analyzed and interpreted the data, wrote and revised the manuscript, and approved the final draft. M.B., C.M., F.B., S.C., and C.P. interpreted the data and reviewed the manuscript. J.P.W., G.B., and C.C. designed the study, revised the manuscript, and approved the final draft.

Acknowledgments

The authors thank all of the team members of the biological and clinical IVF Unit of the Cochin-Port Royal University Hospital center for the assistance that they provided. The authors also gratefully acknowledge Prof. Didier Borderie for his help with biochemistry.

Funding

This study was partially supported by a Merck Biopharma France Research Grant awarded to C.C. and P.S. The funder played no role in the study design, data collection and analysis, decision to publish, or preparation of the manuscript. There was no additional external funding received for this study.

Conflict of interest

None to declare

BIBLIOGRAPHY

Amberg, A., Riefke, B., Schlotterbeck, G., Ross, A., Senn, H., Dieterle, F., Keck, M., 2017. NMR and MS Methods for Metabolomics. Methods Mol. Biol. Clifton NJ 1641, 229–258. https://doi.org/10.1007/978-1-4939-7172-5_13

Atkins, H.M., Bharadwaj, M.S., O'Brien Cox, A., Furdui, C.M., Appt, S.E., Caudell, D.L., 2019. Endometrium and endometriosis tissue mitochondrial energy metabolism in a nonhuman primate model. Reprod. Biol. Endocrinol. 17, 70. https://doi.org/10.1186/s12958-019-0513-8

Bender, K., Walsh, S., Evans, A.C.O., Fair, T., Brennan, L., 2010. Metabolite concentrations in follicular fluid may explain differences in fertility between heifers and lactating cows. Reproduction 139, 1047–1055. https://doi.org/10.1530/REP-10-0068

Boland, N.I., Humpherson, P.G., Leese, H.J., Gosden, R.G., 1994. The effect of glucose metabolism on murine follicle development and steroidogenesis in vitro. Hum. Reprod. 9, 617–623. https://doi.org/10.1093/oxfordjournals.humrep.a138559

Bourdon, M., Santulli, P., Gayet, V., Maignien, C., Marcellin, L., Pocate-Cheriet, K., Chapron, C., 2017. Assisted reproduction technique outcomes for fresh versus deferred cryopreserved day-2 embryo transfer: a retrospective matched cohort study. Reprod. Biomed. Online 34, 248–257. https://doi.org/10.1016/j.rbmo.2016.11.015

Bromer, J.G., Seli, E., 2008. Assessment of embryo viability in assisted reproductive technology: shortcomings of current approaches and the emerging role of metabolomics. Curr. Opin. Obstet. Gynecol. 20, 234–241. https://doi.org/10.1097/GCO.0b013e3282fe723d

Calder, P.C., Yaqoob, P., 1999. Glutamine and the immune system. Amino Acids 17, 227–241. https://doi.org/10.1007/BF01366922

Chapron, C., Bourret, A., Chopin, N., Dousset, B., Leconte, M., Amsellem-Ouazana, D., de Ziegler, D., Borghese, B., 2010a. Surgery for bladder endometriosis: long-term results and concomitant management of associated posterior deep lesions. Hum. Reprod. Oxf. Engl. 25, 884–889. https://doi.org/10.1093/humrep/deq017

Chapron, C., Chopin, N., Borghese, B., Foulot, H., Dousset, B., Vacher-Lavenu, M.C., Vieira, M., Hasan, W., Bricou, A., 2006. Deeply infiltrating endometriosis: pathogenetic implications of the anatomical distribution. Hum. Reprod. Oxf. Engl. 21, 1839–1845. https://doi.org/10.1093/humrep/del079

Chapron, C., Marcellin, L., Borghese, B., Santulli, P., 2019. Rethinking mechanisms, diagnosis and management of endometriosis. Nat. Rev. Endocrinol. 15, 666–682. https://doi.org/10.1038/s41574-019-0245-z

Chapron, C., Pietin-Vialle, C., Borghese, B., Davy, C., Foulot, H., Chopin, N., 2009. Associated ovarian endometrioma is a marker for greater severity of deeply infiltrating endometriosis. Fertil. Steril. 92, 453–457. https://doi.org/10.1016/j.fertnstert.2008.06.003

Chapron, C., Souza, C., de Ziegler, D., Lafay-Pillet, M.-C., Ngô, C., Bijaoui, G., Goffinet, F., Borghese, B., 2010b. Smoking habits of 411 women with histologically proven endometriosis and 567 unaffected women. Fertil. Steril. 94, 2353–2355. https://doi.org/10.1016/j.fertnstert.2010.04.020

Cheng, X., Yang, S., Xu, C., Li, L., Zhang, Y., Guo, Y., Zhang, C., Li, P., Long, M., He, J., 2019. Proanthocyanidins Protect against β-Hydroxybutyrate-Induced Oxidative Damage in Bovine Endometrial Cells. Molecules 24. https://doi.org/10.3390/molecules24030400

Chong, J., Soufan, O., Li, C., Caraus, I., Li, S., Bourque, G., Wishart, D.S., Xia, J., 2018. MetaboAnalyst 4.0: towards more transparent and integrative metabolomics analysis. Nucleic Acids Res. 46, W486–W494. https://doi.org/10.1093/nar/gky310

Chriett, S., Dąbek, A., Wojtala, M., Vidal, H., Balcerczyk, A., Pirola, L., 2019. Prominent action of butyrate over β-hydroxybutyrate as histone deacetylase inhibitor, transcriptional modulator and anti-inflammatory molecule. Sci. Rep. 9, 742. https://doi.org/10.1038/s41598-018-36941-9

Convertini, P., Menga, A., Andria, G., Scala, I., Santarsiero, A., Morelli, M.A.C., Iacobazzi, V., Infantino, V., 2016. The contribution of the citrate pathway to oxidative stress in Down syndrome. Immunology 149, 423–431. https://doi.org/10.1111/imm.12659

Cordeiro, F.B., Cataldi, T.R., Perkel, K.J., Teixeira da Costa, L. do V., Rochetti, R.C., Stevanato, J., Eberlin, M.N., Zylbersztejn, D.S., Cedenho, A.P., Lo Turco, E.G., 2015. Lipidomics analysis of follicular fluid by ESI-MS reveals potential biomarkers for ovarian endometriosis. J. Assist. Reprod. Genet. 32, 1817–1825. https://doi.org/10.1007/s10815-015-0592-1

Cordeiro, F.B., Cataldi, T.R., Teixeira da Costa, L. do V., de Souza, B.Z., Montani, D.A., Fraietta, R., Labate, C.A., Cedenho, A.P., Lo Turco, E.G., 2017. Metabolomic profiling in follicular fluid of patients with infertility-related deep endometriosis. Metabolomics 13, 120. https://doi.org/10.1007/s11306-017-1262-3

Cox-York, K.A., Erickson, C.B., Pereira, R.I., Bessesen, D.H., Van Pelt, R.E., 2017. Region-specific effects of oestradiol on adipose-derived stem cell differentiation in post-menopausal women. J. Cell. Mol. Med. 21, 677–684. https://doi.org/10.1111/jcmm.13011

Da Broi, M.G., Giorgi, V.S.I., Wang, F., Keefe, D.L., Albertini, D., Navarro, P.A., 2018. Influence of follicular fluid and cumulus cells on oocyte quality: clinical implications. J. Assist. Reprod. Genet. 35, 735–751. https://doi.org/10.1007/s10815-018-1143-3

de Ziegler, D., Gayet, V., Aubriot, F.X., Fauque, P., Streuli, I., Wolf, J.P., de Mouzon, J., Chapron, C., 2010. Use of oral contraceptives in women with endometriosis before assisted reproduction treatment improves outcomes. Fertil. Steril. 94, 2796–2799. https://doi.org/10.1016/j.fertnstert.2010.05.056

Dhillon, K.K., Gupta, S., 2020. Biochemistry, Ketogenesis, in: StatPearls. StatPearls Publishing, Treasure Island (FL).
Donnez, J., Binda, M.M., Donnez, O., Dolmans, M.-M., 2016. Oxidative stress in the pelvic cavity and its role in the pathogenesis of endometriosis. Fertil. Steril. 106, 1011–1017. https://doi.org/10.1016/j.fertnstert.2016.07.1075
Duarte, I.F., Gil, A.M., 2012. Metabolic signatures of cancer unveiled by NMR spectroscopy of human biofluids. Prog. Nucl. Magn. Reson. Spectrosc. 62, 51–74. https://doi.org/10.1016/j.pnmrs.2011.11.002
Dumesic, D.A., Meldrum, D.R., Katz-Jaffe, M.G., Krisher, R.L., Schoolcraft, W.B., 2015. Oocyte environment: follicular fluid and cumulus cells are critical for oocyte health. Fertil. Steril. 103, 303–316. https://doi.org/10.1016/j.fertnstert.2014.11.015
Edwards, R.G., 1974. FOLLICULAR FLUID. Reproduction 37, 189–219. https://doi.org/10.1530/jrf.0.0370189
Eriksson, L., Antti, H., Gottfries, J., Holmes, E., Johansson, E., Lindgren, F., Long, I., Lundstedt, T., Trygg, J., Wold, S., 2004. Using chemometrics for navigating in the large data sets of genomics, proteomics, and metabonomics (gpm). Anal. Bioanal. Chem. 380, 419–429. https://doi.org/10.1007/s00216-004-2783-y
Eriksson, L., Trygg, J., Wold, S., 2008. CV-ANOVA for significance testing of PLS and OPLS® models. J. Chemom. 22, 594–600. https://doi.org/10.1002/cem.1187
Fortune, J.E., 1994. Ovarian follicular growth and development in mammals. Biol. Reprod. 50, 225–232. https://doi.org/10.1095/biolreprod50.2.225
Fournier, B., Häring, S., Kaye, A.M., Sömjen, D., 1996. Stimulation of creatine kinase specific activity in human osteoblast and endometrial cells by estrogens and anti-estrogens and its modulation by calciotropic hormones. J. Endocrinol. 150, 275–285. https://doi.org/10.1677/joe.0.1500275
Fukao, T., Lopaschuk, G.D., Mitchell, G.A., 2004. Pathways and control of ketone body metabolism: on the fringe of lipid biochemistry. Prostaglandins Leukot. Essent. Fatty Acids 70, 243–251. https://doi.org/10.1016/j.plefa.2003.11.001
Garrido, N., Navarro, J., Remohí, J., Simón, C., Pellicer, A., 2000. Follicular hormonal environment and embryo quality in women with endometriosis. Hum. Reprod. Update 6, 67–74. https://doi.org/10.1093/humupd/6.1.67
Gosden, R.G., Hunter, R.H., Telfer, E., Torrance, C., Brown, N., 1988. Physiological factors underlying the formation of ovarian follicular fluid. J. Reprod. Fertil. 82, 813–825. https://doi.org/10.1530/jrf.0.0820813
Guerriero, Stefano, Alcázar, J.L., Pascual, M.A., Ajossa, S., Perniciano, M., Piras, A., Mais, V., Piras, B., Schirru, F., Benedetto, M.G., Saba, L., 2018. Deep Infiltrating Endometriosis: Comparison Between 2-Dimensional Ultrasonography (US), 3-Dimensional US, and Magnetic Resonance Imaging. J. Ultrasound Med. Off. J. Am. Inst. Ultrasound Med. 37, 1511–1521. https://doi.org/10.1002/jum.14496
Guerriero, S., Condous, G., van den Bosch, T., Valentin, L., Leone, F.P.G., Van Schoubroeck, D., Exacoustos, C., Installé, A.J.F., Martins, W.P., Abrao, M.S., Hudelist, G., Bazot, M., Alcazar, J.L., Gonçalves, M.O., Pascual, M.A., Ajossa, S., Savelli, L., Dunham, R., Reid, S., Menakaya, U., Bourne, T., Ferrero, S., Leon, M., Bignardi, T., Holland, T., Jurkovic, D., Benacerraf, B., Osuga, Y., Somigliana, E., Timmerman, D., 2016. Systematic approach to sonographic evaluation of the pelvis in women with suspected endometriosis, including terms, definitions and measurements: a consensus opinion from the International Deep Endometriosis Analysis (IDEA) group. Ultrasound Obstet. Gynecol. Off. J. Int. Soc. Ultrasound Obstet. Gynecol. 48, 318–332. https://doi.org/10.1002/uog.15955
Guerriero, S., Saba, L., Pascual, M.A., Ajossa, S., Rodriguez, I., Mais, V., Alcazar, J.L., 2018. Transvaginal ultrasound vs magnetic resonance imaging for diagnosing deep infiltrating

endometriosis: systematic review and meta-analysis. Ultrasound Obstet. Gynecol. Off. J. Int. Soc. Ultrasound Obstet. Gynecol. 51, 586–595. https://doi.org/10.1002/uog.18961
Gull, I., Geva, E., Lerner-Geva, L., Lessing, J.B., Wolman, I., Amit, A., 1999. Anaerobic glycolysis. The metabolism of the preovulatory human oocyte. Eur. J. Obstet. Gynecol. Reprod. Biol. 85, 225–228. https://doi.org/10.1016/s0301-2115(99)00012-3
Guzmán, M., Blázquez, C., 2004. Ketone body synthesis in the brain: possible neuroprotective effects. Prostaglandins Leukot. Essent. Fatty Acids 70, 287–292. https://doi.org/10.1016/j.plefa.2003.05.001
Hosios, A.M., Hecht, V.C., Danai, L.V., Johnson, M.O., Rathmell, J.C., Steinhauser, M.L., Manalis, S.R., Vander Heiden, M.G., 2016. Amino Acids Rather than Glucose Account for the Majority of Cell Mass in Proliferating Mammalian Cells. Dev. Cell 36, 540–549. https://doi.org/10.1016/j.devcel.2016.02.012
Hsiao, K.-Y., Lin, S.-C., Wu, M.-H., Tsai, S.-J., 2015. Pathological functions of hypoxia in endometriosis. Front. Biosci. Elite Ed. 7, 309–321.
Hsu, A.L., Townsend, P.M., Oehninger, S., Castora, F.J., 2015. Endometriosis may be associated with mitochondrial dysfunction in cumulus cells from subjects undergoing in vitro fertilization-intracytoplasmic sperm injection, as reflected by decreased adenosine triphosphate production. Fertil. Steril. 103, 347-352.e1. https://doi.org/10.1016/j.fertnstert.2014.11.002
Huhtinen, K., Desai, R., Ståhle, M., Salminen, A., Handelsman, D.J., Perheentupa, A., Poutanen, M., 2012. Endometrial and Endometriotic Concentrations of Estrone and Estradiol Are Determined by Local Metabolism Rather than Circulating Levels. J. Clin. Endocrinol. Metab. 97, 4228–4235. https://doi.org/10.1210/jc.2012-1154
Jacob, D., Deborde, C., Lefebvre, M., Maucourt, M., Moing, A., 2017. NMRProcFlow: a graphical and interactive tool dedicated to 1D spectra processing for NMR-based metabolomics. Metabolomics 13, 36. https://doi.org/10.1007/s11306-017-1178-y
Jana, S.K., Dutta, M., Joshi, M., Srivastava, S., Chakravarty, B., Chaudhury, K., 2013. 1H NMR based targeted metabolite profiling for understanding the complex relationship connecting oxidative stress with endometriosis. BioMed Res. Int. 2013, 329058. https://doi.org/10.1155/2013/329058
Kanikarla-Marie, P., Jain, S.K., 2015. Role of Hyperketonemia in Inducing Oxidative Stress and Cellular Damage in Cultured Hepatocytes and Type 1 Diabetic Rat Liver. Cell. Physiol. Biochem. Int. J. Exp. Cell. Physiol. Biochem. Pharmacol. 37, 2160–2170. https://doi.org/10.1159/000438573
Karaer, A., Tuncay, G., Mumcu, A., Dogan, B., 2019. Metabolomics analysis of follicular fluid in women with ovarian endometriosis undergoing in vitro fertilization. Syst. Biol. Reprod. Med. 65, 39–47. https://doi.org/10.1080/19396368.2018.1478469
Kerner, J., Hoppel, C.L., 2004. Ketogenesis, in: Lennarz, W.J., Lane, M.D. (Eds.), Encyclopedia of Biological Chemistry. Elsevier, New York, pp. 505–507. https://doi.org/10.1016/B0-12-443710-9/00346-X
Knox, W.E., 1955. [38] Enzymes involved in conversion of tyrosine to acetoacetate: A. l-Tyrosine-Oxiding system of liver, in: Methods in Enzymology. Academic Press, pp. 287–300. https://doi.org/10.1016/S0076-6879(55)02202-7
Knox, W.E., LeMay-Knox, M., 1951. The oxidation in liver of l-tyrosine to acetoacetate through p-hydroxyphenylpyruvate and homogentisic acid. Biochem. J. 49, 686–693.
Kurepa, D., Pramanik, A.K., Kakkilaya, V., Caldito, G., Groome, L.J., Bocchini, J.A., Jain, S.K., 2012. Elevated acetoacetate and monocyte chemotactic protein-1 levels in cord blood of infants of diabetic mothers. Neonatology 102, 163–168. https://doi.org/10.1159/000339286
Le Foll, C., Levin, B.E., 2016. Fatty acid-induced astrocyte ketone production and the control of food intake. Am. J. Physiol. - Regul. Integr. Comp. Physiol. 310, R1186–R1192.

https://doi.org/10.1152/ajpregu.00113.2016
Maignien, C., Santulli, P., Chouzenoux, S., Gonzalez-Foruria, I., Marcellin, L., Doridot, L., Jeljeli, M., Grange, P., Reis, F.M., Chapron, C., Batteux, F., 2019. Reduced alpha-2,6 sialylation regulates cell migration in endometriosis. Hum. Reprod. 34, 479–490. https://doi.org/10.1093/humrep/dey391
Marianna, S., Alessia, P., Susan, C., Francesca, Caprio, Angela, S., Francesca, Capone, Antonella, N., Patrizia, I., Nicola, C., Emilio, C., 2017. Metabolomic profiling and biochemical evaluation of the follicular fluid of endometriosis patients. Mol. Biosyst. 13, 1213–1222. https://doi.org/10.1039/c7mb00181a
Markley, J.L., Brüschweiler, R., Edison, A.S., Eghbalnia, H.R., Powers, R., Raftery, D., Wishart, D.S., 2017. The future of NMR-based metabolomics. Curr. Opin. Biotechnol., Analytical biotechnology 43, 34–40. https://doi.org/10.1016/j.copbio.2016.08.001
Martinez-Outschoorn, U.E., Lin, Z., Whitaker-Menezes, D., Howell, A., Lisanti, M.P., Sotgia, F., 2012. Ketone bodies and two-compartment tumor metabolism: stromal ketone production fuels mitochondrial biogenesis in epithelial cancer cells. Cell Cycle Georget. Tex 11, 3956–3963. https://doi.org/10.4161/cc.22136
MEIBOOM, S., GILL, D., 1958. MODIFIED SPIN-ECHO METHOD FOR MEASURING NUCLEAR RELAXATION TIMES. Rev. Sci. Instrum. 29, 688–691. https://doi.org/10.1063/1.1716296
Morelli, M.A.C., Iuliano, A., Schettini, S.C.A., Petruzzi, D., Ferri, A., Colucci, P., Viggiani, L., Cuviello, F., Ostuni, A., 2019. NMR metabolic profiling of follicular fluid for investigating the different causes of female infertility: a pilot study. Metabolomics 15, 19. https://doi.org/10.1007/s11306-019-1481-x
Ngô, C., Chéreau, C., Nicco, C., Weill, B., Chapron, C., Batteux, F., 2009. Reactive oxygen species controls endometriosis progression. Am. J. Pathol. 175, 225–234. https://doi.org/10.2353/ajpath.2009.080804
Nisenblat, V., Bossuyt, P.M.M., Farquhar, C., Johnson, N., Hull, M.L., 2016. Imaging modalities for the non-invasive diagnosis of endometriosis. Cochrane Database Syst. Rev. 2, CD009591. https://doi.org/10.1002/14651858.CD009591.pub2
Noster, J., Persicke, M., Chao, T.-C., Krone, L., Heppner, B., Hensel, M., Hansmeier, N., 2019. Impact of ROS-Induced Damage of TCA Cycle Enzymes on Metabolism and Virulence of Salmonella enterica serovar Typhimurium. Front. Microbiol. 10. https://doi.org/10.3389/fmicb.2019.00762
O'Gorman, A., Wallace, M., Cottell, E., Gibney, M.J., McAuliffe, F.M., Wingfield, M., Brennan, L., 2013. Metabolic profiling of human follicular fluid identifies potential biomarkers of oocyte developmental competence. Reproduction 146, 389–395. https://doi.org/10.1530/REP-13-0184
Ohata, Y., Harada, T., Miyakoda, H., Taniguchi, F., Iwabe, T., Terakawa, N., 2008. Serum interleukin-8 levels are elevated in patients with ovarian endometrioma. Fertil. Steril. 90, 994–999. https://doi.org/10.1016/j.fertnstert.2007.07.1355
O'Neill, L.A.J., 2011. A critical role for citrate metabolism in LPS signalling. Biochem. J. 438, e5-6. https://doi.org/10.1042/BJ20111386
Orazov, M., Yevseyevich, R., Isaakovich, I., Хамошина, M., Borisovna, S., 2019. Oocyte quality in women with infertility associated endometriosis. Gynecol. Endocrinol. 35, 24–26. https://doi.org/10.1080/09513590.2019.1632088
Owen, O.E., Hanson, R.W., 2004. Ketone Bodies, in: Martini, L. (Ed.), Encyclopedia of Endocrine Diseases. Elsevier, New York, pp. 125–136. https://doi.org/10.1016/B0-12-475570-4/01447-5
Palin, S.L., McTernan, P.G., Anderson, L.A., Sturdee, D.W., Barnett, A.H., Kumar, S., 2003. 17Beta-estradiol and anti-estrogen ICI:compound 182,780 regulate expression of lipoprotein

lipase and hormone-sensitive lipase in isolated subcutaneous abdominal adipocytes. Metabolism. 52, 383–388. https://doi.org/10.1053/meta.2003.50088
Piñero-Sagredo, E., Nunes, S., de Los Santos, M.J., Celda, B., Esteve, V., 2010. NMR metabolic profile of human follicular fluid. NMR Biomed. 23, 485–495. https://doi.org/10.1002/nbm.1488
Redding, G.P., Bronlund, J.E., Hart, A.L., 2008. Theoretical investigation into the dissolved oxygen levels in follicular fluid of the developing human follicle using mathematical modelling. Reprod. Fertil. Dev. 20, 408–417. https://doi.org/10.1071/rd07190
Regiani, T., Cordeiro, F.B., da Costa, L. do V.T., Salgueiro, J., Cardozo, K., Carvalho, V.M., Perkel, K.J., Zylbersztejn, D.S., Cedenho, A.P., Lo Turco, E.G., 2015. Follicular fluid alterations in endometriosis: label-free proteomics by MS(E) as a functional tool for endometriosis. Syst. Biol. Reprod. Med. 61, 263–276. https://doi.org/10.3109/19396368.2015.1037025
Revelli, A., Piane, L.D., Casano, S., Molinari, E., Massobrio, M., Rinaudo, P., 2009. Follicular fluid content and oocyte quality: from single biochemical markers to metabolomics. Reprod. Biol. Endocrinol. RBE 7, 40. https://doi.org/10.1186/1477-7827-7-40
Sampson, J., 1927. Peritoneal endometriosis due to menstrual dissemination of endometrial tissue into the peritoneal cavity. Am J Obstet Gynecol 442–69.
Sanchez, A.M., Vanni, V.S., Bartiromo, L., Papaleo, E., Zilberberg, E., Candiani, M., Orvieto, R., Viganò, P., 2017. Is the oocyte quality affected by endometriosis? A review of the literature. J. Ovarian Res. 10. https://doi.org/10.1186/s13048-017-0341-4
Sanchez, A.M., Viganò, P., Somigliana, E., Panina-Bordignon, P., Vercellini, P., Candiani, M., 2014. The distinguishing cellular and molecular features of the endometriotic ovarian cyst: from pathophysiology to the potential endometrioma-mediated damage to the ovary. Hum. Reprod. Update 20, 217–230. https://doi.org/10.1093/humupd/dmt053
Santulli, P., Chouzenoux, S., Fiorese, M., Marcellin, L., Lemarechal, H., Millischer, A.-E., Batteux, F., Borderie, D., Chapron, C., 2015. Protein oxidative stress markers in peritoneal fluids of women with deep infiltrating endometriosis are increased. Hum. Reprod. 30, 49–60. https://doi.org/10.1093/humrep/deu290
Scutiero, G., Iannone, P., Bernardi, G., Bonaccorsi, G., Spadaro, S., Volta, C.A., Greco, P., Nappi, L., 2017. Oxidative Stress and Endometriosis: A Systematic Review of the Literature. Oxid. Med. Cell. Longev. 2017. https://doi.org/10.1155/2017/7265238
Shi, X., Li, D., Deng, Q., Peng, Z., Zhao, C., Li, Xiaobing, Wang, Z., Li, Xinwei, Liu, G., 2016. Acetoacetic acid induces oxidative stress to inhibit the assembly of very low density lipoprotein in bovine hepatocytes. J. Dairy Res. 83, 442–446. https://doi.org/10.1017/S0022029916000546
Shi, X., Li, X., Li, D., Li, Y., Song, Y., Deng, Q., Wang, J., Zhang, Y., Ding, H., Yin, L., Zhang, Y., Wang, Z., Li, X., Liu, G., 2014. ß-Hydroxybutyrate Activates the NF-κB Signaling Pathway to Promote the Expression of Pro-Inflammatory Factors in Calf Hepatocytes. Cell. Physiol. Biochem. 33, 920–932. https://doi.org/10.1159/000358664
Sutton, M.L., Gilchrist, R.B., Thompson, J.G., 2003. Effects of in-vivo and in-vitro environments on the metabolism of the cumulus–oocyte complex and its influence on oocyte developmental capacity. Hum. Reprod. Update 9, 35–48. https://doi.org/10.1093/humupd/dmg009
Trygg, J., Wold, S., 2002. Orthogonal projections to latent structures (O-PLS). J. Chemom. 16, 119–128. https://doi.org/10.1002/cem.695
van den Berg, R.A., Hoefsloot, H.C., Westerhuis, J.A., Smilde, A.K., van der Werf, M.J., 2006. Centering, scaling, and transformations: improving the biological information content of metabolomics data. BMC Genomics 7, 142. https://doi.org/10.1186/1471-2164-7-142
Van den Bosch, T., Van Schoubroeck, D., 2018. Ultrasound diagnosis of endometriosis and

adenomyosis: State of the art. Best Pract. Res. Clin. Obstet. Gynaecol. 51, 16–24. https://doi.org/10.1016/j.bpobgyn.2018.01.013
Wallace, M., Cottell, E., Gibney, M.J., McAuliffe, F.M., Wingfield, M., Brennan, L., 2012. An investigation into the relationship between the metabolic profile of follicular fluid, oocyte developmental potential, and implantation outcome. Fertil. Steril. 97, 1078-1084.e8. https://doi.org/10.1016/j.fertnstert.2012.01.122
Wang, C.-H., Wu, S.-B., Wu, Y.-T., Wei, Y.-H., 2013. Oxidative stress response elicited by mitochondrial dysfunction: implication in the pathophysiology of aging. Exp. Biol. Med. Maywood NJ 238, 450–460. https://doi.org/10.1177/1535370213493069
Warburg, O., 1956. On the Origin of Cancer Cells. Science 123, 309–314.
Williams, N.C., O'Neill, L.A.J., 2018. A Role for the Krebs Cycle Intermediate Citrate in Metabolic Reprogramming in Innate Immunity and Inflammation. Front. Immunol. 9. https://doi.org/10.3389/fimmu.2018.00141
Wingfield, M., Macpherson, A., Healy, D.L., Rogers, P.A.W., 1995. Cell proliferation is increased in the endometrium of women with endometriosis *. Fertil. Steril. 64, 340–346. https://doi.org/10.1016/S0015-0282(16)57733-4
Wishart, D.S., Tzur, D., Knox, C., Eisner, R., Guo, A.C., Young, N., Cheng, D., Jewell, K., Arndt, D., Sawhney, S., Fung, C., Nikolai, L., Lewis, M., Coutouly, M.-A., Forsythe, I., Tang, P., Shrivastava, S., Jeroncic, K., Stothard, P., Amegbey, G., Block, D., Hau, D.D., Wagner, J., Miniaci, J., Clements, M., Gebremedhin, M., Guo, N., Zhang, Y., Duggan, G.E., Macinnis, G.D., Weljie, A.M., Dowlatabadi, R., Bamforth, F., Clive, D., Greiner, R., Li, L., Marrie, T., Sykes, B.D., Vogel, H.J., Querengesser, L., 2007. HMDB: the Human Metabolome Database. Nucleic Acids Res. 35, D521-526. https://doi.org/10.1093/nar/gkl923
Xia, J., Psychogios, N., Young, N., Wishart, D.S., 2009. MetaboAnalyst: a web server for metabolomic data analysis and interpretation. Nucleic Acids Res. 37, W652–W660. https://doi.org/10.1093/nar/gkp356
Xu, B., Guo, N., Zhang, X., Shi, W., Tong, X., Iqbal, F., Liu, Y., 2015. Oocyte quality is decreased in women with minimal or mild endometriosis. Sci. Rep. 5, 10779. https://doi.org/10.1038/srep10779
Yuan, L., Sheng, X., Willson, A.K., Roque, D.R., Stine, J.E., Guo, H., Jones, H.M., Zhou, C., Bae-Jump, V.L., 2015. Glutamine promotes ovarian cancer cell proliferation through the mTOR/S6 pathway. Endocr. Relat. Cancer 22, 577–591. https://doi.org/10.1530/ERC-15-0192
Zarghami, N., Giai, M., Yu, H., Roagna, R., Ponzone, R., Katsaros, D., Sismondi, P., Diamandis, E.P., 1996. Creatine kinase BB isoenzyme levels in tumour cytosols and survival of breast cancer patients. Br. J. Cancer 73, 386–390. https://doi.org/10.1038/bjc.1996.66
Zhou, W.-J., Zhang, J., Yang, H.-L., Wu, K., Xie, F., Wu, J.-N., Wang, Y., Yao, L., Zhuang, Y., Xiang, J.-D., Zhang, A.-J., He, Y.-Y., Li, M.-Q., 2019. Estrogen inhibits autophagy and promotes growth of endometrial cancer by promoting glutamine metabolism. Cell Commun. Signal. 17, 99. https://doi.org/10.1186/s12964-019-0412-9
Zondervan, K.T., Cardon, L.R., Kennedy, S.H., 2002. What makes a good case-control study? Design issues for complex traits such as endometriosis. Hum. Reprod. Oxf. Engl. 17, 1415–1423. https://doi.org/10.1093/humrep/17.6.1415

Table 1. Baseline characteristics of the patients.

Patient characteristics	Endometriosis (n = 9)	Control (n = 7)	P-value[d]
Age (years)[a]	35.7 ± 5.1	37.4 ± 3.5	0.393
BMI (kg/m^2)[a]	22.5 ± 3.1	23.2 ± 3.7	0.606
Parity[a]	0.1 ± 0.4	0.6 ± 0.9	0.362
Gravidity[a]	0.1 ± 0.4	0.4 ± 0.8	0.407
Infertility			0.771
Primary	7 (77.8%)	5 (71.4%)	
Secondary	2 (22.2%)	2 (28.6%)	
Length of infertility (months) [a]	32.8 ± 11.4	34.3 ± 18.6	0.679
Day 3 ovarian reserve			
FSH (IU/mL) [a]	6.4 ± 3.3	6.7 ± 2.9	0.957
LH (IU/mL) [a]	4.3 ± 2.8	4.4 ± 1.1	0.707
Estradiol (pg/mL) [a]	86.2 ± 83.5	49.1 ± 21.1	0.397
AMH (ng/mL) [a]	2.9 ± 1.6	2.9 ± 1.3	0.634
Antral Follicular Count [a]	16.8 ± 9.6	20.9 ± 11.3	0.457
Surgical classification of endometriosis *(n, %)* [b]			
DIE with associated OMA	5 (55.6%)	NA	NA
DIE without associated OMA	4 (44.4%)	NA	NA
Intestinal DIE	5 (55.5%)	NA	NA
Total number of DIE lesions [a]	2.8 ± 1.1	NA	NA
Follicular volume (mL)	1.9 ± 0.7	1.9 ± 0.8	0.874
Oocyte retrieved	12.6 ± 8.9	9.6 ± 6.3	0.632

Note: BMI, body mass index; FSH, follicle-stimulating hormone; LH, luteinizing hormone; AMH, anti-Müllerian hormone; OMA, ovarian endometrioma; DIE, deep infiltrating endometriosis; NA, not applicable

[a] *The data are presented as means ± the standard deviation*

[b] *According to a previously published surgical classification for deep infiltrating endometriosis (Chapron et al., 2006)*

[d] *The statistical analysis was performed using Fisher's exact test or Pearson's chi-square for the qualitative variables and the Mann–Whitney U test for the quantitative variables,*

Statistical significance: $p < 0.05$

Table 2. Baseline characteristics of the OMA+ and the OMA- DIE patients.

Patient characteristics	**OMA+ (n = 5)**	**OMA- (n = 4)**
Age (years)[a]	34 ± 1.7	37.8 ± 7.4
BMI (kg/m^2)[a]	22.4 ± 2.6	22.6 ± 4
Parity[a]	0	0.25 ± 0.5
Gravidity[a]	0	0
Infertility		
Primary	4 (80%)	3 (75%)
Secondary	1 (20%)	1 (25%)
Length of infertility (months) [a]	28.5 ± 11.4	37 ± 11.1
Day 3 ovarian reserve		
FSH (IU/mL) [a]	6.2 ± 1.1	6.8 ± 5.3
LH (IU/mL) [a]	3.4 ± 3	5.5 ± 2.4
Estradiol (pg/mL) [a]	37.2 ± 21.4	147.5 ± 94.8
AMH (ng/mL) [a]	3.5 ± 2	2.1 ± 0.5
Antral Follicular Count [a]	17.6 ± 9.6	15.8 ± 11.1
Follicular Volume (mL)	1.6 ± 0.4	2.4 ± 0.8
Oocyte retrieved	14 ± 12	10.8 ± 3.3

Note: BMI, body mass index; FSH, follicle-stimulating hormone; LH, luteinizing hormone; AMH, anti-Müllerian hormone; OMA, ovarian endometrioma; DIE, deep infiltrating endometriosis; NA, not applicable

[a] The data are presented as means ± the standard deviation

Figure 1. Representative 500 MHz ^{1}H-NMR (nuclear magnetic resonance) spectrum of a deep infiltrating endometriosis follicular fluid (FF) sample.

Note: TYR, tyrosine; GLN, glutamine; ALA, Alanine; THR, threonine; ILE, isoleucine. ^{1}H-NMR spectrum of a follicular fluid sample from a patient with endometriosis, obtained at 300 K on a spectrometer operating at a proton frequency of 500.45 MHz. The assignment of statistically relevant metabolites is indicated above their corresponding NMR peaks.

Figure 2: Endometriosis (n = 50) vs. Control (n = 29): Univariate analysis.

The results are presented as boxplots showing statistically significant differences ($p < 0.05$) in metabolite concentrations obtained from the Student's *t*-test using MetaboAnalyst (Chong *et al.*, 2018; Xia *et al.*, 2009).

The data are presented as medians, interquartile ranges, and individual values. The average value for each group is also indicated as a yellow diamond.

Note: C, control samples; DIE, deep infiltrating endometriosis samples

2A. Boxplots corresponding to glucose, lactate, and pyruvate metabolites.

2B. Boxplots corresponding to ketone body and lipid metabolites. *Note: FA, fatty acids*

2C. Boxplots corresponding to amino acid, citrate, and creatine metabolites.

Note: TYR, tyrosine; ALA, alanine; THR, threonine; ILE, isoleucine

Figure 3: Endometriosis (n = 50) vs. Control (n = 29): Supervised multivariate analysis.

The data were obtained using SIMCA software.

3A: Score plot of the orthogonal partial least square discriminant analysis (OPLS-DA) of the follicular fluid samples. Full and dashed-line circles correspond to the presence and absence of endometrioma, respectively, within the DIE group.

The corresponding quality factors were as follows: $R^2X = 0.839$, $R^2Y = 0.844$, and $Q^2 = 0.697$. The OPLS-DA model was validated with a p-value of 6.09×10^{-13}, obtained using CV-ANOVA.

Note: C, control samples; DIE, deep infiltrating endometriosis

3B. Variable importance in projection (VIP) score plot for the multivariate analysis of the follicular fluid samples.

Note: THR, threonine; FA, fatty acid

The variables contributing the most to the group discrimination in the OPLS-DA model were plotted according to their VIP score, i.e., the weight of each variable in the group separation. The chemical shift center of the corresponding variable NMR signal is indicated on the X-axis. The same metabolite can have different NMR signals, thus giving rise to different buckets. The variables were sorted according to their VIP score, with a threshold of 1 to consider the variables that have a significant power on the separation of groups in the OPLS-DA model. The metabolites that exhibited increased levels in patients with endometriosis are indicated by a black box; those that had reduced levels are indicated by a white box. All of the metabolites were also validated in the univariate analysis ($p < 0.05$).

Figure 4: DIE with endometrioma (OMA+, n = 25) vs. DIE with no endometrioma (OMA-, n = 25) vs. Control (n = 29): Univariate analysis.

The results are presented as boxplots showing statistically significant differences in metabolite concentrations obtained from a one-way ANOVA for comparisons between the three groups ($p < 0.05$), whereas the Student's *t*-test was used for the comparison of each combination of pairs ($*p < 0.05$, $**p < 0.01$, and $***p < 0.001$). The data were obtained using MetaboAnalyst (Chong *et al.*, 2018; Xia *et al.*, 2009).

The data are presented as medians, interquartile ranges, and individual values. The average value for each group is also indicated as a yellow diamond.

Note: C, control samples; OMA-, deep infiltrating endometriosis (DIE) with no endometrioma samples; OMA+, DIE endometriosis with endometrioma samples

4A. Boxplots corresponding to ketone body and glycerol metabolites.

4B. Boxplots corresponding to glucose, lactate, and pyruvate metabolites.

4C. Boxplots corresponding to amino acids, succinate, and creatine metabolites.

Note: ILE, isoleucine; TYR, tyrosine, ALA, alanine; THR, threonine; GLN, glutamine

Figure 5 (in Supplementary files): DIE with endometrioma (OMA+, n = 25) vs. DIE with no endometrioma (OMA-, n = 25) vs. Control (n = 29): Supervised multivariate analysis.

Score plot of the orthogonal partial least square discriminant analysis (OPLS-DA) of the follicular fluid samples using SIMCA software.

The corresponding quality factors were as follows: $R^2X = 0.87$, $R^2Y = 0.858$, and $Q^2 = 0.756$.

The OPLS-DA model was validated with a p-value of 1.9×10^{-14}, obtained using CV-ANOVA.

Note: C, control samples; OMA-, DIE without associated endometrioma samples; OMA+, DIE with associated endometrioma sample.

Figure 6: Schematic representation of the putative metabolic pathways altered in the follicular fluid from patients with endometriosis.

Note: FA, fatty acids; KB, ketone bodies; P-Creatine, phosphocreatine; ROS, reactive oxygen species; TCA, tricarboxylic acid cycle

Large grey arrows indicate the variation in metabolite concentrations in the follicular fluid (FF) from patients with DIE compared with their concentration in control samples.

A dysfunctional TCA cycle could explain the observed accumulation of threonine observed in the DIE FF samples. Citrate, which would no longer be used in this pathway, can be converted into oxaloacetate in the cytoplasm, thereby giving rise to reactive oxygen species (ROS) as well as an inflammatory response.

In the FF of endometriosis patients with no endometrioma, glucose is directed toward pyruvate and lactate production by the anaerobic glycolysis pathway (blue). Conversely, the presence of an endometrioma is characterized by a predilection toward other energetic pathways, such as lipolysis followed by fatty acid β-oxidation, thereby resulting in the release of glycerol and ketone bodies (red).

Figure 1.

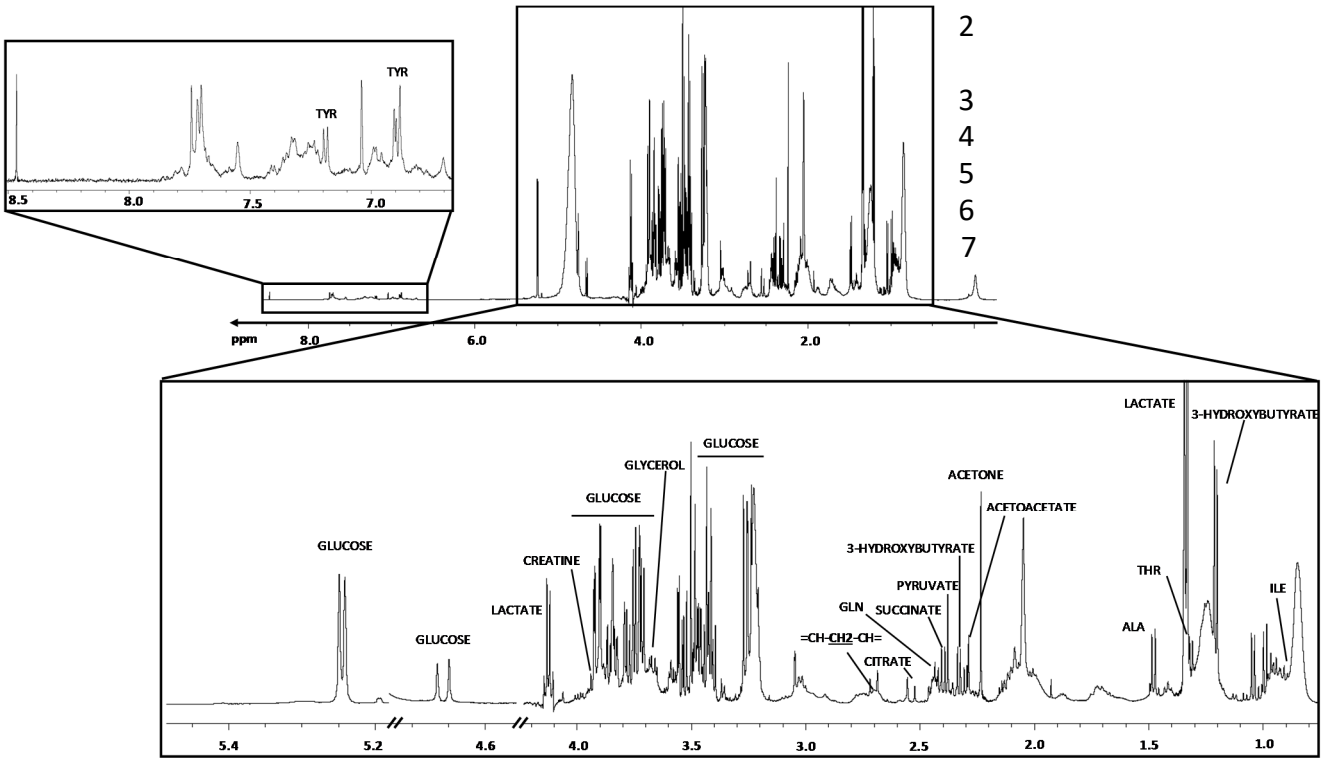
TYR
TYR
8.5
8.0
7.5
7.0
ppm
8.0
6.0
4.0
2.0
GLUCOSE
GLUCOSE
GLUCOSE
GLYCEROL
GLUCOSE
CREATINE
LACTATE
GLUCOSE
GLN
SUCCINATE
=CH-CH2-CH=
CITRATE
PYRUVATE
3-HYDROXYBUTYRATE
ACETONE
ACETOACETATE
ALA
THR
LACTATE
3-HYDROXYBUTYRATE
ILE
5.4
5.2
4.6
4.0
3.5
3.0
2.5
2.0
1.5
1.0

Figure 2

2A

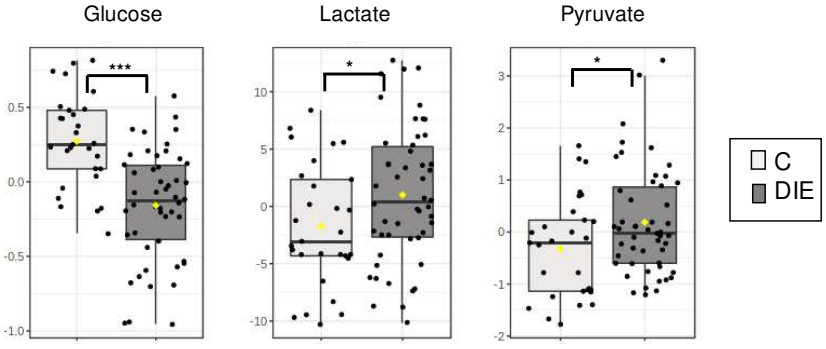

2B

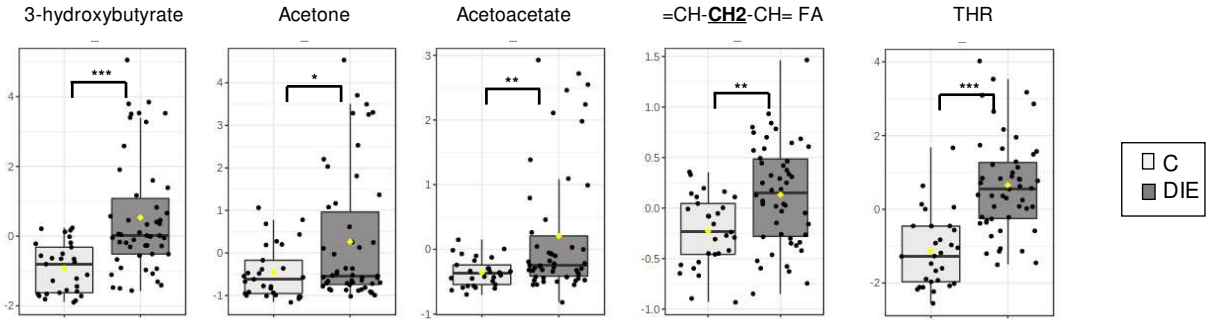

2C

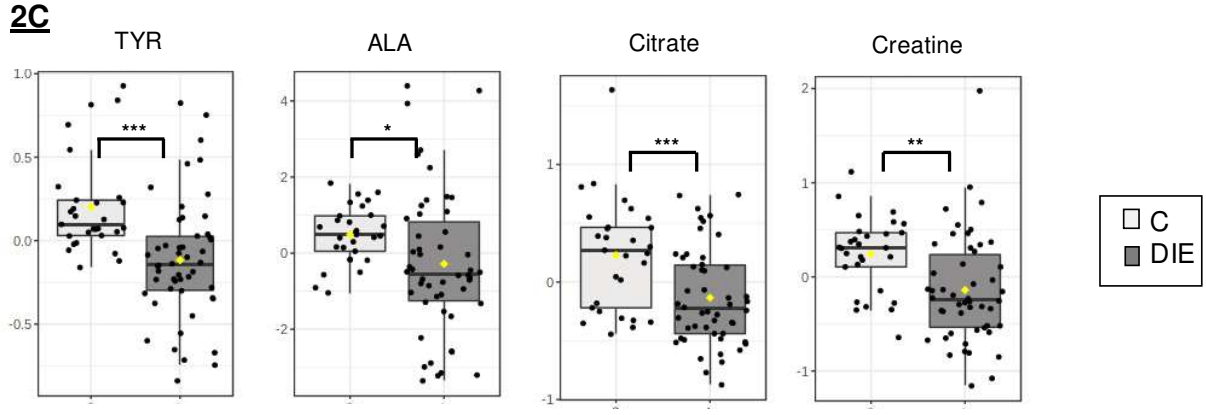

*p-value < 0.05

**p-value < 0.01

***p-value < 0.001

37 **Figure 3**

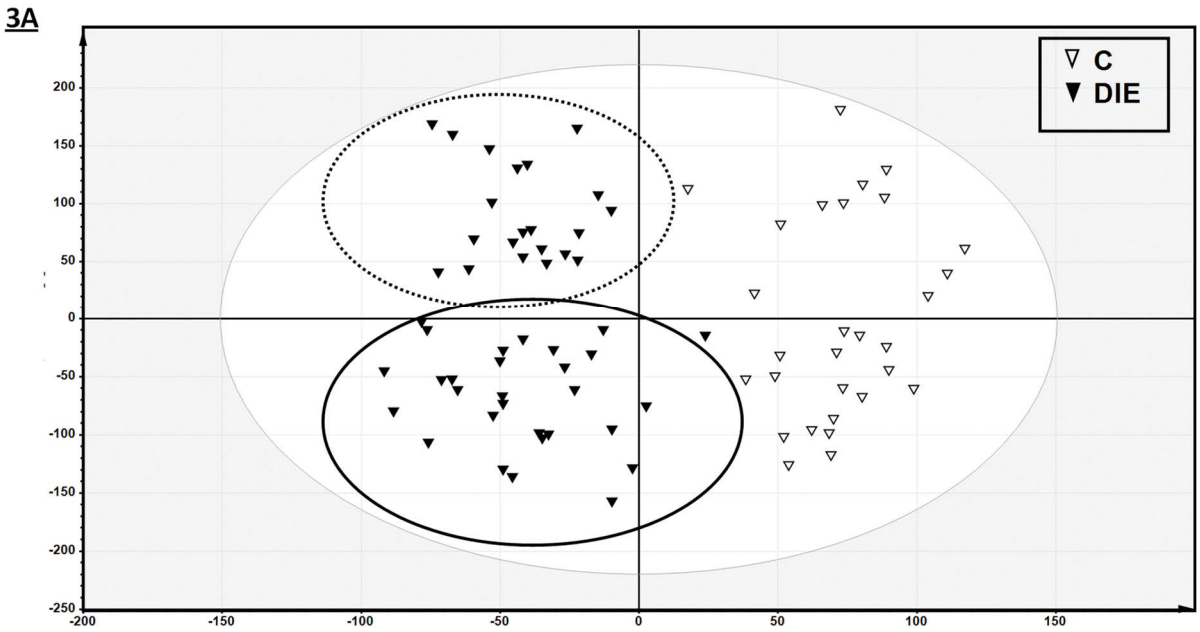

38

39

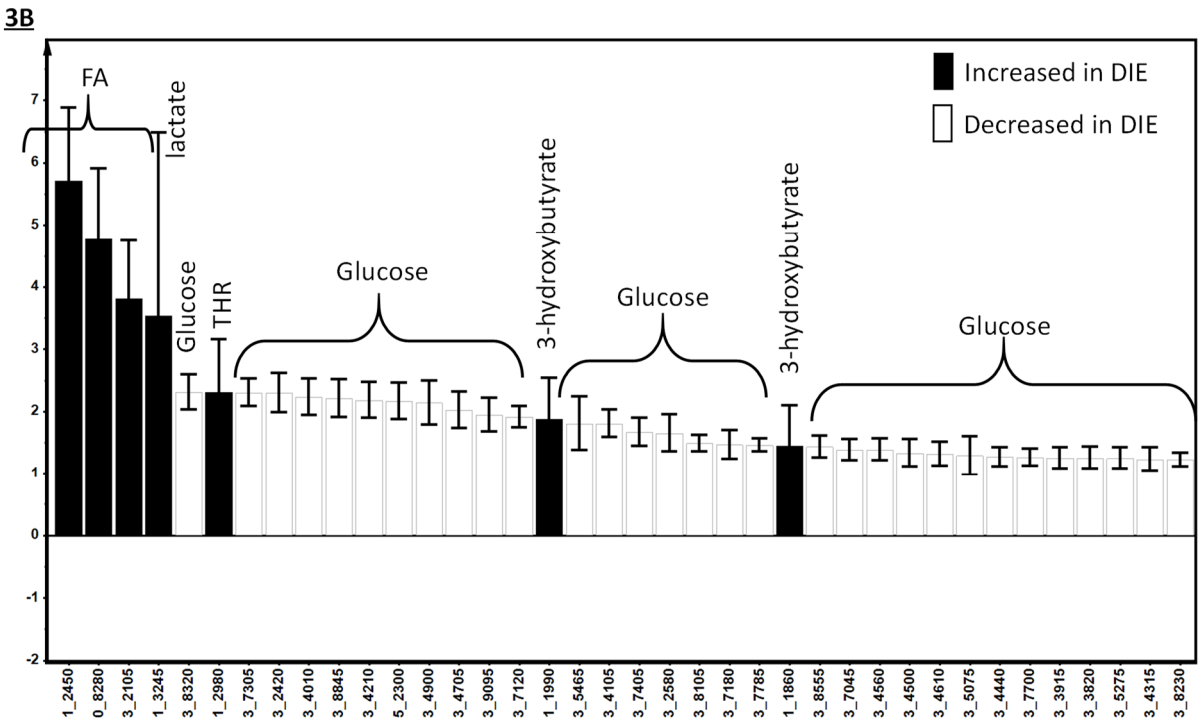

40

Figure 4

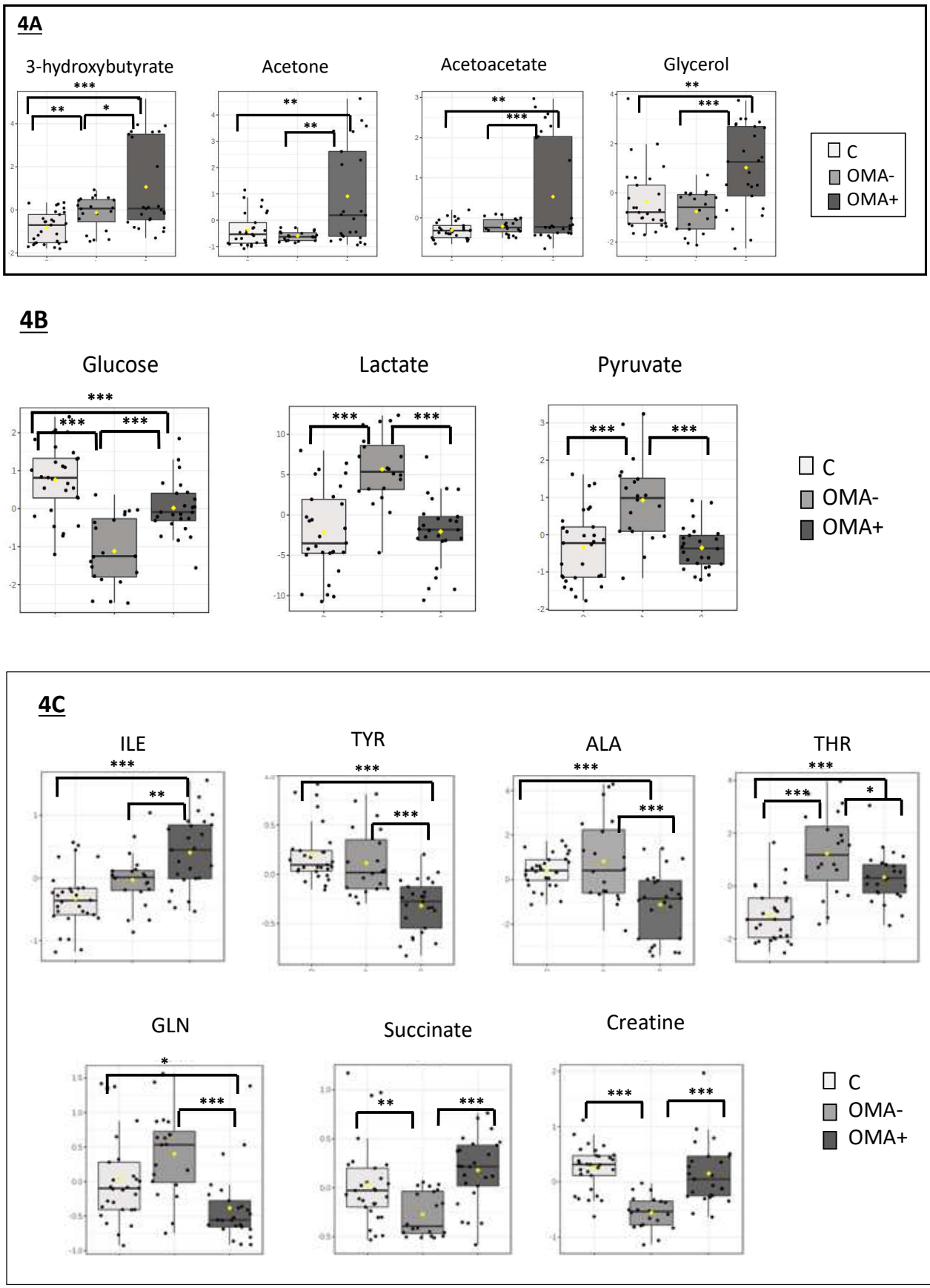
4A
3-hydroxybutyrate
Acetone
Acetoacetate
Glycerol
C
OMA-
OMA+
4B
Glucose
Lactate
Pyruvate
C
OMA-
OMA+
4C
ILE
TYR
ALA
THR
GLN
Succinate
Creatine
C
OMA-
OMA+

Figure 5

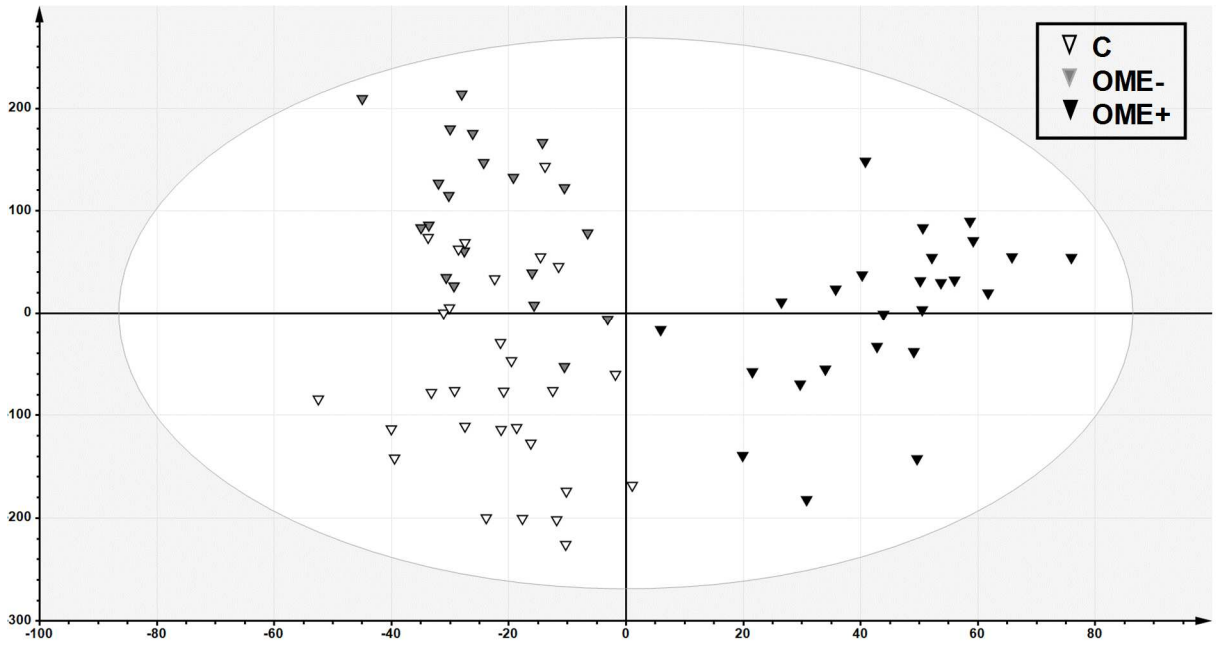

Figure 6

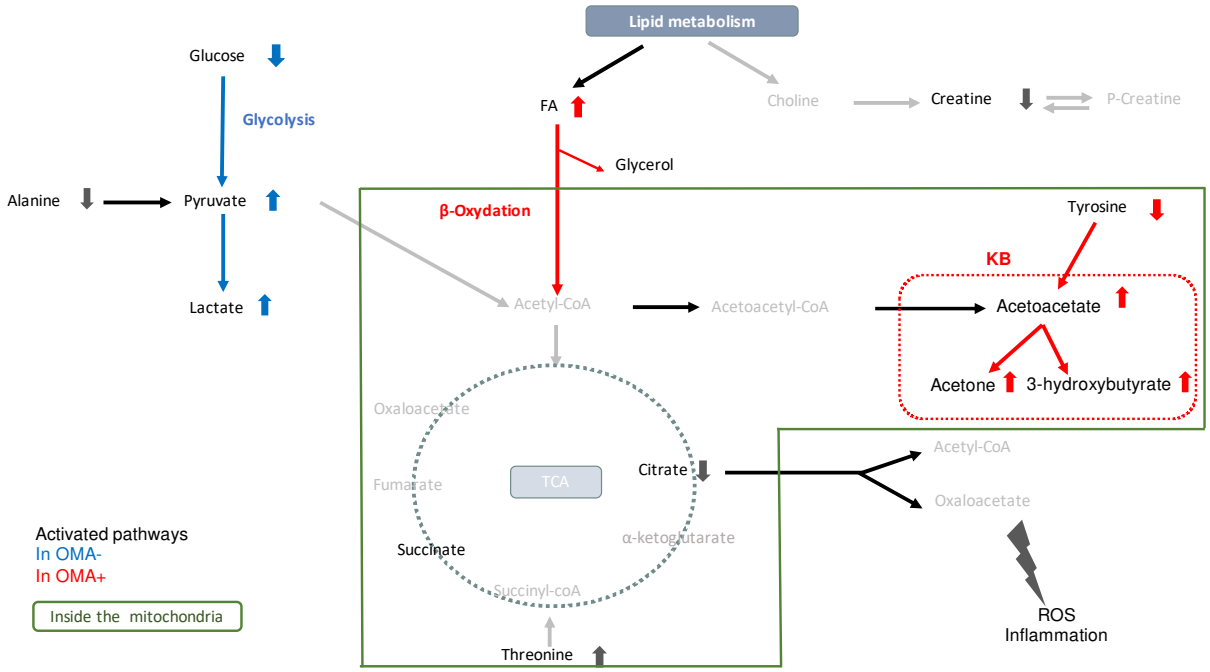
Lipid metabolism
Glucose
Glycolysis
FA
Choline
Creatine
P-Creatine
Glycerol
Alanine
Pyruvate
Lactate
β-Oxydation
Tyrosine
KB
Acetyl-CoA
Acetoacetyl-CoA
Acetoacetate
Acetone
3-hydroxybutyrate
Oxaloacetate
Fumarate
TCA
Citrate
Acetyl-CoA
Oxaloacetate
Succinate
α-ketoglutarate
Succinyl-coA
Threonine
ROS
Inflammation
Activated pathways
In OMA-
In OMA+
Inside the mitochondria